

## DISTORTION OF STEEL PLATE GIRDERS DUE TO HOT-DIP GALVANIZING

**Authors:** Kien Nguyen<sup>1</sup>, Reza Nasouri<sup>2</sup>, Caroline Bennett<sup>1</sup>, Adolfo Matamoros<sup>2</sup>, Jian Li<sup>1</sup>, Arturo Montoya<sup>2</sup>

<sup>1</sup> Department of Civil, Environmental and Architectural Engineering, University of Kansas, Lawrence, Kansas.

<sup>2</sup> Department of Civil and Environmental Engineering, University of Texas at San Antonio, San Antonio, Texas

### **Abstract:**

Hot-dip galvanizing can be an attractive choice as a corrosion protection system for steel bridge designers and owners. During the hot-dip galvanizing process, steel bridge components are submerged in an approximately 840F bath of zinc to form a metallurgically-bonded zinc coating. The existence of larger kettle sizes has made it possible to hot-dip galvanize larger girders and trusses for bridge construction. However, distortion of structural elements during and immediately after the galvanizing process remains a concern, especially with welded steel plate girders. Generally, this distortion is caused by the thermal stresses induced by high temperature of the zinc bath, which may further interact with residual stresses produced during member fabrication. A lack of understanding of plate girder susceptibility to distortion results in designers and owners hesitating to choose hot-dip galvanizing for their bridges.

This paper describes a finite element study on the distortion of welded steel plate girders. The non-linear simulations model a continuous procedure, which includes welding and hot-dip galvanizing processes. The finite element analysis software Abaqus with the plug-in Abaqus Welding Interface (AWI) was used to simulate the welding process. The as-welded component was subjected to the hot-dip galvanizing process through a thermal simulation specified using an Abaqus user-subroutine. The parameters of the study were the geometry of plate girders and hot-dip galvanizing practices such as dipping angle, and dipping and removing velocity. The results of this study will provide guidance to engineers, galvanizers, and fabricators to minimize steel plate girder distortion so that they can more confidently use hot-dip galvanizing to protect their bridges.

**Keywords:** Distortion, steel plate girders, welding, hot-dip galvanizing.

# Introduction

## Background

In the hot-dip galvanizing process, steel components are dipped into a kettle of liquid zinc to form a metallurgically-bonded zinc coating to prevent corrosion, as shown in Figure 1. According to the American Galvanizers Association (AGA), the average kettle length in North America is 40 ft (with some as large as 65 ft), the average width is 5-11 ft, and depths range from 6 to 12 ft [1]. The existence of these large kettle sizes has made it possible to hot-dip galvanize larger structures such as welded steel plate girders. However, distortion of girders due to the heating and cooling associated with the hot-dip galvanizing process is a great concern that can cause bridge designers, fabricators, and owners to hesitate before utilizing this method.

Distortion of plate girders during galvanizing is a complicated problem because it depends on many factors such as structure geometry, fabrication techniques, and galvanizing practices. Although concerns regarding plate girder distortion are not new, there remains little information on how to prevent this particular problem from occurring. While ASTM A384 [2] provides some information regarding causes and suggested corrections regarding the distortion of general steel assemblies, the guidance is less clear when it comes to plate girders, which are welded assemblies of elements with different thickness. Questions that must be addressed are:

- What are the characteristics of the distortion behavior that occurs in welded plate girders throughout the galvanizing process?
- How do geometry, welding operations, and galvanizing operations affect the distortion behavior of welded plate girders?

According to the American Galvanizers Association (AGA), the flange-to-web thickness ratio of plate girders should be no more than 3 to 1 to avoid distortion of the web [1] during

galvanizing. In addition, the AGA recommends adding stiffeners, reducing dwelling time, and using plate thicknesses larger than  $\frac{1}{4}$  in. Cresdee, et al. [3] investigated the effect of girder dimensions and dipping parameters on several forms of two-dimensional distortion (e.g. bowing, sweep, and buckling, shown in Figure 1) during hot-dip galvanizing. The results showed that thicker flanges and deeper webs reduced the bowing of I-girders, thicker and shorter webs reduced the risk of web buckling, faster dipping reduced distortion, and dipping orientation strongly affected non-symmetric girders such as T- and C- shapes. In their study Cresdee et al. [3] did not consider the effects of welding, which may strongly affect girder distortions through the imparted initial imperfections and residual stresses. Furthermore, due to the limited capabilities of 2-D finite element models, three-dimensional distortion effects, such as twisting, were not considered.

## Objective and Scope

The objective of this study was to investigate the distortion behavior of welded plate girders during galvanizing, evaluating the influence of the following parameters on girder distortion: flange and web dimensions, dipping speed, and dipping angle. The study was performed using 3-D finite element models, using sequentially-coupled thermomechanical analyses for the welding and galvanizing processes. A common welding sequence used to fabricate plate girders was explicitly simulated, calculating imperfections associated with the welding process, residual stresses, and residual strains. Results from the welding simulation were used as the initial configuration for two parametric studies evaluating the effect of girder dimensions and galvanizing parameters on girder distortion behavior. Finally, some recommendations are presented to prevent distortion of steel plate girders due to the galvanizing process.

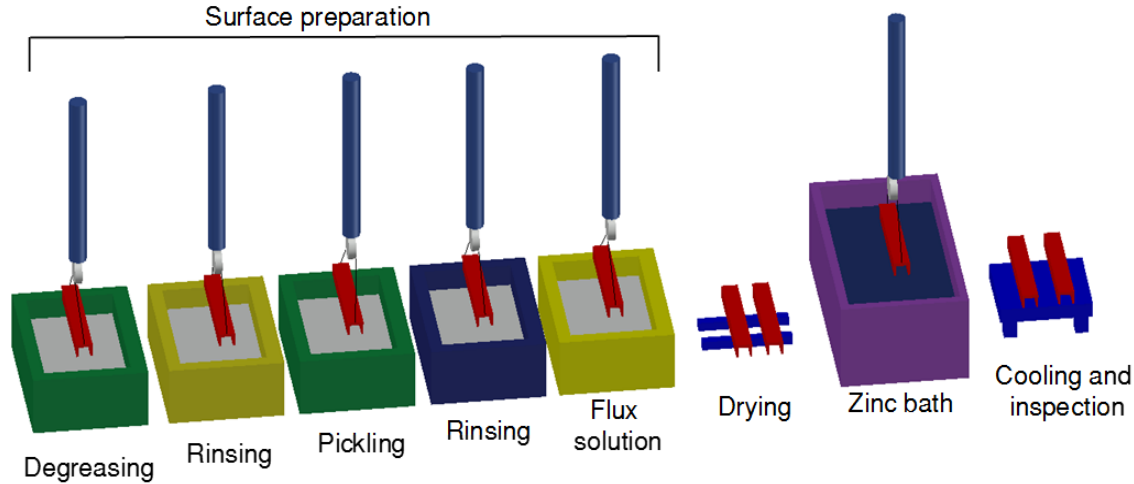


**Figure 1. Hot-dip galvanizing process (adapted from the AGA [1]).**

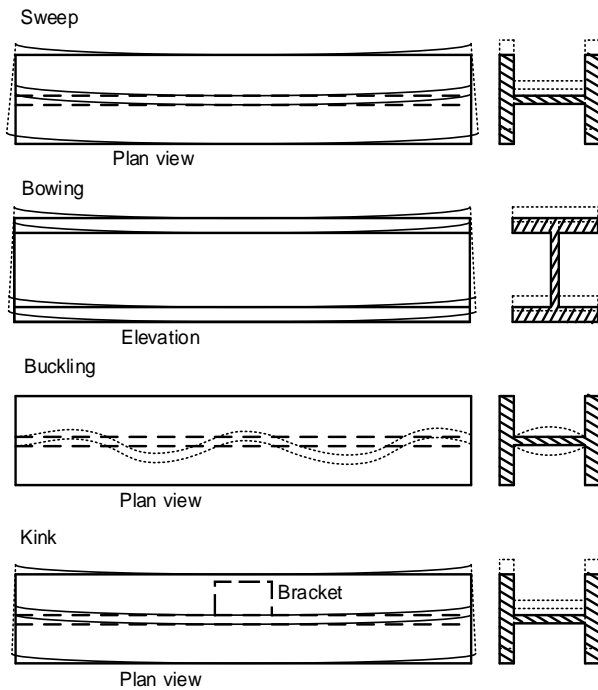


**Figure 2. Typical forms of distortion in girders (adapted from Cresdee, et al. [3]).**

## Finite Element Models

### General Description

In this work, a three-dimensional model was developed using the commercial software

Abaqus 2017, using a sequentially-coupled thermal-stress analysis to capture the cumulative effect of both welding and galvanizing processes on plate girders. The loading sequence began with a nonlinear heat transfer analysis that simulated the welding sequence and the galvanizing process. The calculated temperature fields were then imposed on the beam section to calculate stress and strain fields. Temperature-dependent thermal and mechanical properties of S355JR steel (equivalent to ASTM A572-50) were sourced from Peric, et al. [4]. In addition to being temperature-dependent, the material model for steel was elastic with linear kinematic hardening in the inelastic range [5].

A total of eight models, described in Table 1, were evaluated in this study. Model 1 was identified as the “baseline” model (flanges 12”x3/4”, web 36”x3/8”). Models 2, 3, and 4 were used to study the effect of flange and web thicknesses on girder distortion, while Models 5, 6, 7, and 8 were used to investigate the effect of galvanizing dipping speed and angle.

A description of the welding process, hot-dip galvanizing process, and mesh configuration is presented in the following. It should be noted that the galvanizing timeline was slightly different for the models within the suite, to accommodate differences in the amount of time required for cooling to ambient temperature after

galvanizing in models with different geometry,

or for

**Table 1. Matrix of models in this study.**

Model	Significance	Flange	Web	Dipping/removing speed (in./min)	Dipping angle (°)
1	Baseline	12"x3/4"	36"x3/8"	24	4
2	Flange thickness (+)	12"x1"	36"x3/8"	24	4
3	Flange thickness (++)	12"x5/4"	36"x3/8"	24	4
4	Web thickness (+)	12"x3/4"	36"x1/2"	24	4
5	Dipping speed (+)	12"x3/4"	36"x3/8"	48	4
6	Dipping speed (++)	12"x3/4"	36"x3/8"	240	4
7	Dipping angle (-)	12"x3/4"	36"x3/8"	24	1
8	Dipping angle (+)	12"x3/4"	36"x3/8"	24	15

completion of the dipping and removing processes in models with different dipping speed or angle. In the following descriptions, the timeline is specific to that of the baseline model.

All models consisted of a plate girder with a length of approximately 12 ft (3600 mm). While this is considerably shorter than typical bridge girders, it was a necessary compromise considering the high computational cost of these models. While girder length is likely to affect the distortion of bridge girders, a length of 12 ft was sufficient to explore differences in the distortion characteristics between models.

### Welding Simulation Methodology

The welding simulation was performed using the plug-in Abaqus Welding Interface, a utility developed by SIMULIA (AWI 2017-1). A full description of the analysis methodology and numerical steps used in the AWI modeling

routine can be found in the AWI Users' Manual [6] and previous studies performed by Nguyen, et al. [7, 8]. A depiction of the welding and galvanizing procedures applied in this study is presented in Figure 3. The web-to-flange welding sequence consisted of placing two web-to-flange welds (1A and 1B) simultaneously on the right side of the girder web, followed by placing two web-to-flange welds (2A and 2B) simultaneously on the left side of the girder web. This sequence simulated welding of the plate girder in lay-down position. The welding speed was  $v = 28$  in./min for all models. The heat convective coefficient in air was  $h_{air} = 3.39699E-6$  Btu/in<sup>2</sup>/s/R [4, 9, 10], the effective emissivity was  $\epsilon = 0.9$ , and the Stefan-Boltzmann constant was  $\sigma = 3.3063E-015$  Btu/s/in<sup>2</sup>/R<sup>4</sup>. Room temperature (air temperature) was specified to be 70°F.

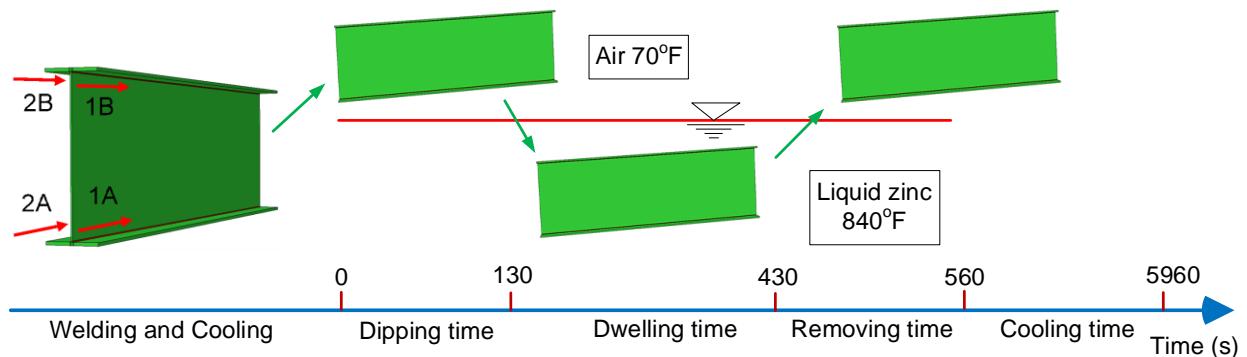


**Figure 3. Simulation of welding and hot-dip galvanizing processes on the baseline model.**

The temperature of the welding torch in the AWI utility was selected as 2732°F (slightly higher than the melting temperature of steel, 2642°F), the weld segment length was 3.15 in., and a ramping option of 100% was chosen. The selection of these parameters were based on a study performed by Nguyen, et al. [7]. These parameters generated a heat input of 40 kJ/in, which is in the common range of heat input of 30-65 kJ/in for large structures such as transmission poles and bridge girders [11]. After the welding process was completed, the simulated girder was allowed to cool for 3600 s before the galvanizing sequence was initiated in the model. This amount of time allowed the girder to cool down approximately to air temperature.

### Galvanizing Simulation Methodology

The thermal and mechanical analyses for the hot-dip galvanizing process were embedded in the model after the welding simulation was completed. An Abaqus user-subroutine, *FILM*, was developed to simulate the external temperature field acting on the girder as it is dipped, held, and extracted from a galvanizing kettle, as illustrated in Figure 3. The *FILM* subroutine created a reference plane which moved up and down the girder model at the dipping velocity. The portion of the girder below the reference plane was assigned parameters representing contact with liquid zinc; the portion above the reference plane was assigned parameters representing contact with air. While steel parts were in contact with liquid zinc in the galvanizing bath, convection between the molten zinc and the structural component was considered to be the primary mode of heat transfer, while radiation and conduction were assumed negligible. The heat convective coefficient used where the girder was in contact with liquid zinc was  $h_{zinc} = 458.59365$  Btu/in<sup>2</sup>/s/R, and was  $h_{air} = 3.39699E-6$  Btu/in<sup>2</sup>/s/R where the girder was in contact with air; both of these coefficients were derived experimentally by Cresdee, et al. [3].

The air temperature was set to 70°F, and the liquid zinc temperature was set to 842°F. Dipping and removing speeds in the baseline

model were 24 in./min. The girder section was modeled as being dipped with an angle of 4°. The girder was held fully submerged in the bath for 300 s (referred to as dwell time). These galvanizing parameters were chosen based on common practice. The total duration of the galvanizing process in the baseline model, including dipping, dwelling, and extraction, was 560 s. After extraction, the girder model was allowed to cool in-air until its temperature was approximately equal to the air temperature, for an additional 5400 s.

### Meshing and Boundary Conditions

The mesh configuration was designed based on the results from a mesh sensitivity study performed for Model 1. The girder web had two elements through a thickness of 3/8 in., while the girder flanges had three elements through the thickness of 3/4 in., as shown in Figure 4. Typical element sizes used in the mesh were 0.19 x 0.25 x 0.31 in. for the web, and 0.28 x 0.25 x 0.31 in. for the flange. Model 1 had a total of 249,300 elements and 356,290 nodes. Eight-node linear heat transfer brick elements (DC3D8) were used for the thermal analysis, while eight-node linear brick elements (C3D8) were used for the stress analysis. Mesh sizes for the other models were similar to those used in Model 1. This practice was adopted to ensure that results would be comparable between models.

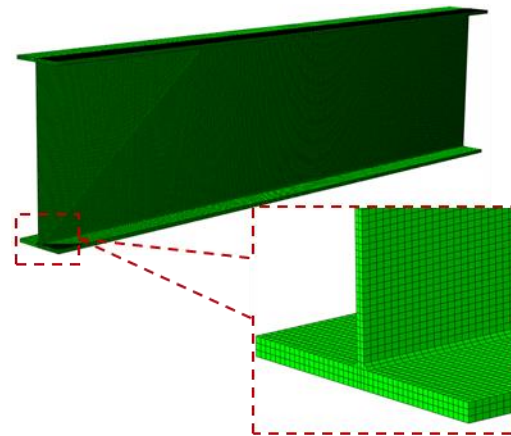


**Figure 4. Meshing of the baseline model.**

In the 3-D simulations of the welding and galvanizing processes, rigid body motion of the

girder was avoided by applying constraints at six different points (Figure 5) [12]. It is important that the placement of these constraints does not restrain the girder from deforming under applied thermal loads. The locations of the six constraint points used in this study have been used by many other researchers, including Deng and Murakawa [13], Kleineck [14], Heinze, et al. [15], Gannon, et al. [16], and Fu, et al. [17]. In this study, different boundary conditions were applied for the welding and hot-dip galvanizing processes, as shown in Figure 5. Boundary conditions for the welding process appear different from welding in the lay-down position, but the effect should remain the same. For the galvanizing process, boundary conditions were to simulate the handling based on common practices. Gravity body force was not applied because its effect is negligible during the welding and galvanizing processes. Results showed that the applied constraints prevented rigid body motion of the girder models without generating significant reactions at the assigned nodes.

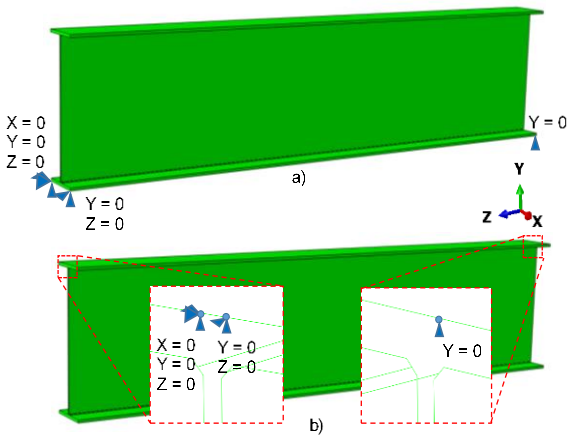


**Figure 5. Boundary conditions applied during: (a) welding process, and (b) galvanizing process.**

## Results and Discussion

The first part of this section presents the results from the baseline model (Model 1), which are useful for characterizing the distortion behavior of the girder during and after the hot-dip

galvanizing process. The second part presents the results from the parametric studies, which were used to investigate the effects of girder geometry and galvanizing practices on plate girder distortion. Finally, a discussion on the potential for cracking based on the calculated distortions is provided.

### Results from the baseline model – understanding the distortion behavior

Calculated temperature and deformation of the baseline plate girder (Model 1) at different times during galvanizing are presented in Figure 6, in columns (a) and (b), respectively. In Figure 6, time  $t=0$  s represents the start of the hot-dip galvanizing process, as shown in Figure 3. At  $t=0$  s, the girder was subject only to the residual stresses/strains and deformations induced by the welding process.

Times of 42, 66, and 96 s presented in Figure 3 correspond to the state of the girder at different points during the dipping process. During dipping, the beam distorted due to differences between the deformation of the bottom portion, expanding while submerged in the molten zinc, and the top portion, still exposed to air. This uneven expansion created a bending deformation in the beam section, which combined with the imperfections and residual stresses/strains induced by the welding process, generated a twisting deformation mode in the girder, with a peak deformation of 5.7 in. at  $t=42$  s. The twisting rapidly disappeared as the girder was further submerged, leading to the release of residual stress. At  $t=96$  s, the simulated zinc surface passed mid-height of the web and produced a large expansion of the portion of the web below the zinc surface, which was constrained by the remaining of the girder. This condition placed the web in longitudinal compression, causing it to undergo web buckling. This web buckling gradually reduced when the girder was fully submerged into the simulated kettle, but some deformations remained, as shown in the buckled areas at

t=150 and 560 s. These deformation patterns were caused by inelastic deformation of the web.

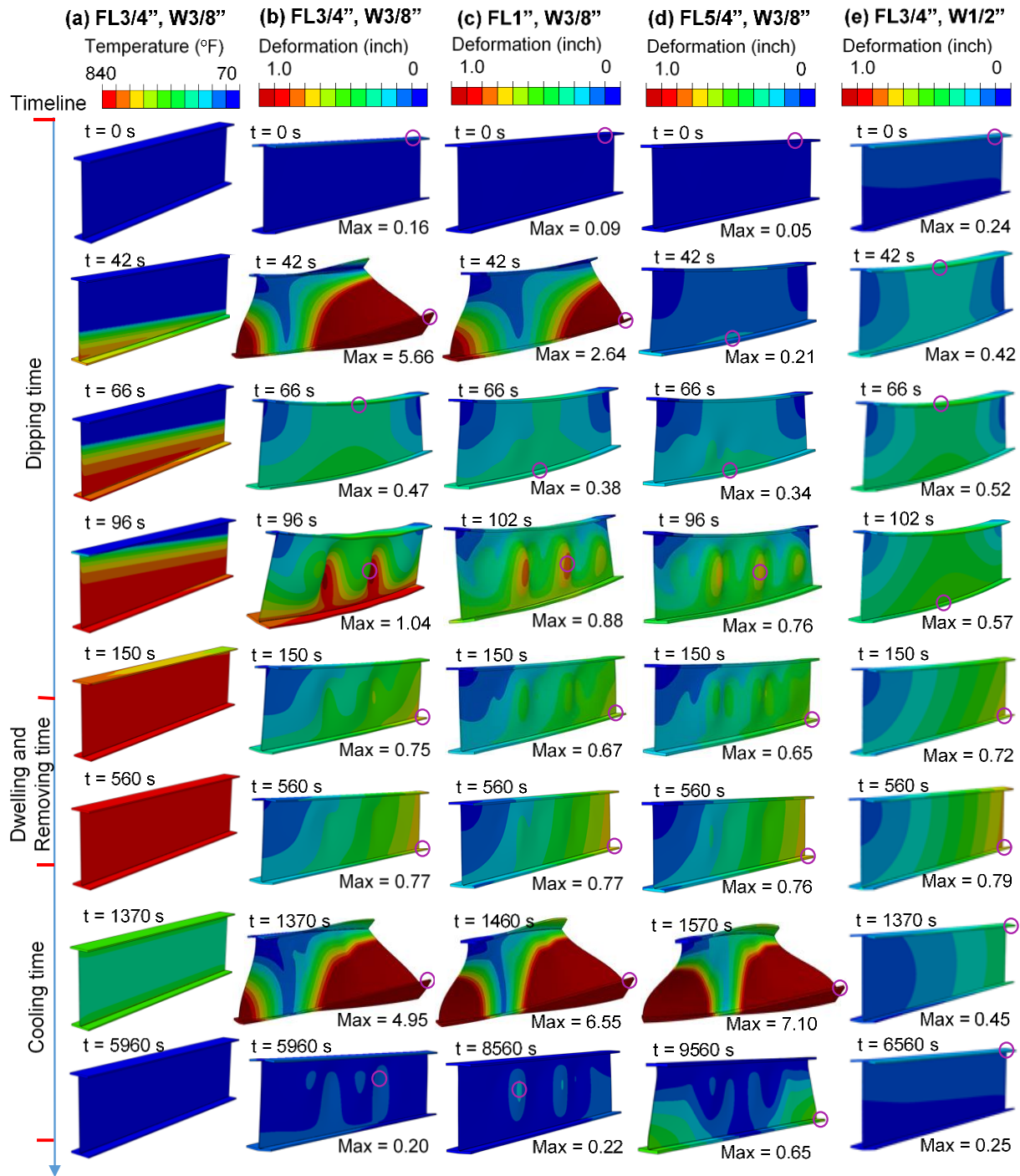


**Figure 6. Evolution of temperature and deformation: (a) Temperature in Model 1; (b) Deformation in Model 1; (c) Deformation in Model 2; (d) Deformation in Model 3; (e) Deformation in Model 4. All deformations are shown 10x for clarity.**

During the cooling period after extraction from the simulated zinc bath, the girder sustained another cycle of twisting, starting at approximately 300 s after removal of the girder from the galvanizing kettle. This twisting distortion was largest (4.95 in.) at approximately  $t=1370$  s, or 810 s after removal from the kettle. The cause of this twisting was the uneven contraction of the web and flanges during this time. The girder reached room temperature after approximately one and a half hours in the cooling phase. The “final” deformed shape of the girder, achieved at  $t=5960$  s is shown in Figure 6 amplified by a factor of 10. While the web buckling pattern is still apparent in the final configuration, the deformation magnitudes were significantly smaller than the peaks during the hot-dip galvanizing process.

### Effect of girder geometry

In addition to the baseline model, Figure 6 shows the deformation results for models with different section dimensions. Flange thickness was increased to 1 in. and 1 ¼ in., and web thickness to ½ in., as presented in columns (c), (d), and (e), respectively. It was found that in general, increasing flange thickness exacerbated distortion effects, while increasing web thickness reduced the tendency of the girder web to buckle. Increasing flange thickness helped reduce residual deformation induced by the welding process, and resulted in less twisting (model with 1 in. thick flanges) or even negligible twisting (model with 1 ¼ in. thick flanges) during the dipping stage, as shown by deformations at  $t=42$  s. However, twisting deformations during the cooling time after galvanizing were worse for these cases than for the model with ¾ in. thick flanges. Peak twisting deformations reached 6.6 in. and 7.1 in. for 1 in. thick and 1 ¼ in. thick flanges, respectively, compared with 4.95 in. of twisting deformation in the baseline model. Increasing the web thickness to ½ in. dramatically reduced the

tendency of the girder to buckle or twist. As shown in column (e) of Figure 6, twisting and web buckling were negligible for this model, even though this model sustained a larger residual deformation induced by the welding process than the others.

Figure 7 shows a different view of the final deformed shapes (deformations amplified 20x) for the four cases in which geometric parameters were varied. As shown in (a), (b) and (c), the distortion increased with increasing flange thickness. On the contrary, deformations decreased with increasing web thickness.

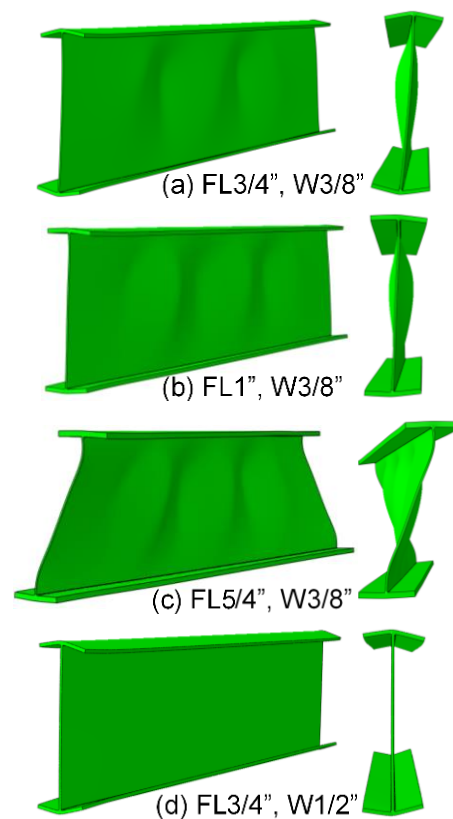


**Figure 7. Effect of geometry on the final deformed shapes (amplified 20x): (a) Model 1, (b) Model 2, (c) Model 3 and (d) Model 4.**

To quantify distortion of the plate girders, three distortion parameters were considered: web out-of-flatness, flange warpage angle, and girder twist angle, each defined in Figure 8. The first two parameters were adapted from the welding code AWS D1.1/D1.1M:2010 [18], while the

third was specific to this study. The effects of web and flange thickness on the three distortion parameters are presented in Figure 9, in the form of the flange-to-web thickness ratio. According to AWS D1.1/D1.1M:2010 Table D.1, statically-loaded girder webs without intermediate stiffeners, for any web thickness and the web depth of 36 in. used in this study, the tolerance for flatness is 1/4 in. All of the out-of-flatness values computed in the four models met this limit. Also according to the AWS D1.1/D1.1M:2010 Figure C-5.7, flange warpage  $\Delta$  should be less than or equal to  $b_f(\text{in.})/100$  or 1/4 in., whichever is greater, where  $b_f$  is the flange width. For all models in this study, the flange widths were 12 in., which led to a tolerance of 1/4 in. for flange warpage, or a flange warpage angle of 2.4 deg. Therefore, the warpage angles post-galvanizing for the four cases were acceptable according to the AWS limits.

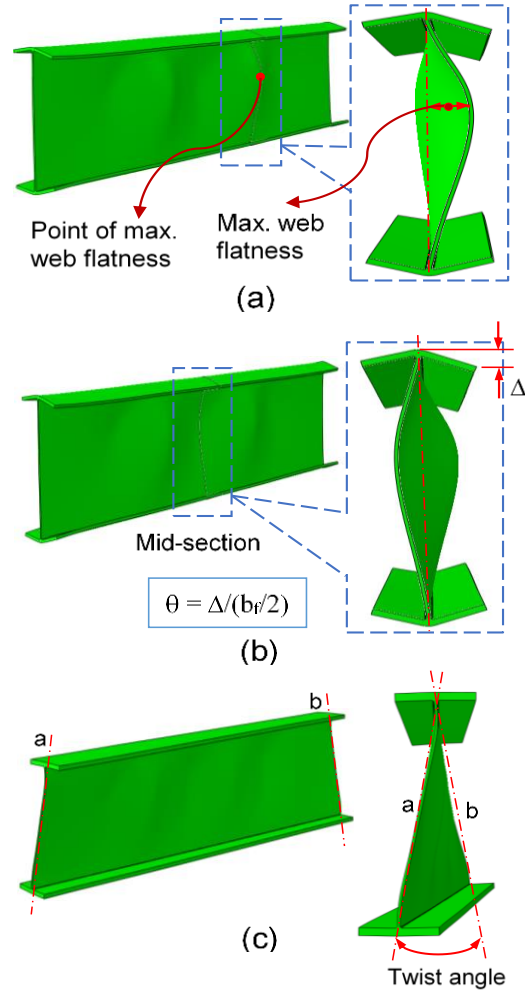


**Figure 8. Distortion parameters: (a) web out-of-flatness, (b) flange warpage angle, and (c) twist angle**

Generally, increasing the thickness ratio increased the web out-of-flatness and twist angle, but decreased the flange warpage angle. These results support the AGA's recommendation of maintaining a thickness ratio of 3 or less between the flange and web dimensions.

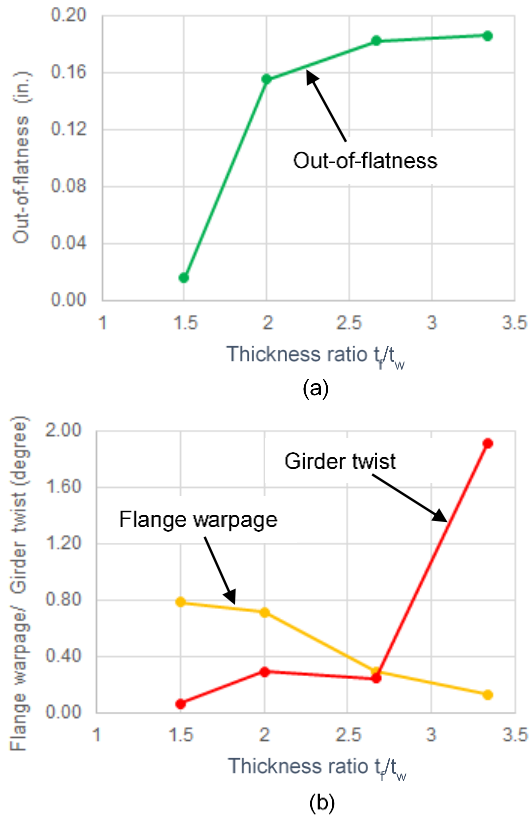
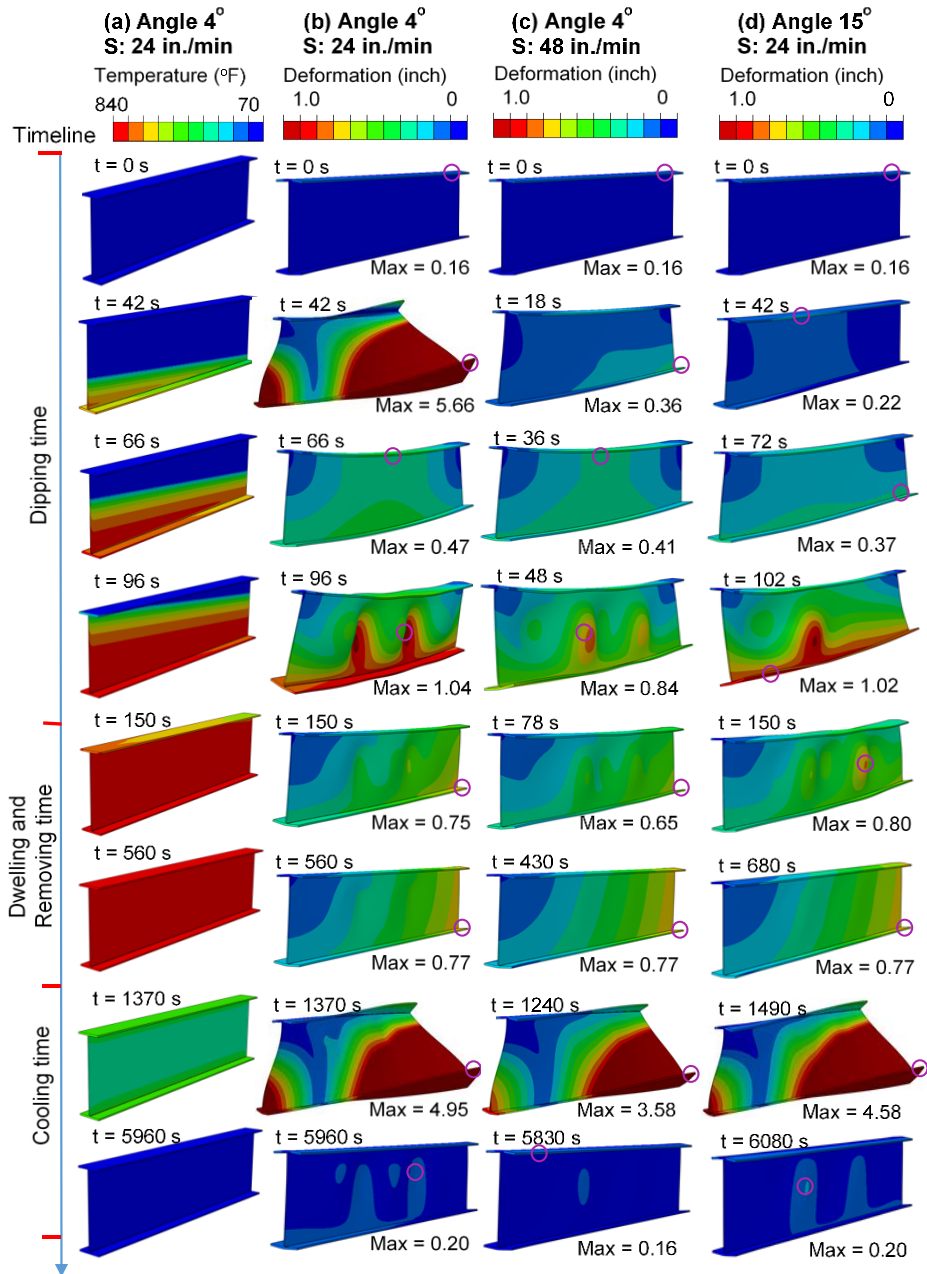


**Figure 9. Effect of flange-to-web thickness ratio on (a) out-of-flatness, (b) flange warpage, and (c) girder twist.**

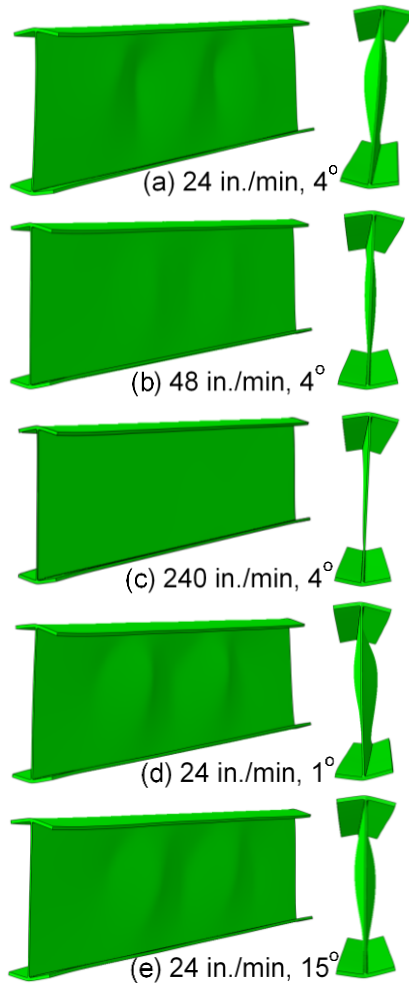
### Effect of hot-dip galvanizing practices

Figure 10 shows the deformation evolution of the baseline model for different dipping speeds and dipping angles. Generally, increasing dipping speed or angle decreased distortion, although the level of influence of these two parameters was different. For example, the model with the faster dipping speed of 48 in./min generated a maximum twisting deformation of 3.58 in. while cooling after galvanizing, while the model with a dipping angle of 15° experienced a maximum deformation of 4.58 in. at the same critical point. Both of these magnitudes were less than the 4.95 in. calculated for the baseline model.

Figure 11 presents the effects of the dipping speed and angle on the final deformed shape of the plate girder at the end of the cooling period, when the girder temperature was approximately equal to room temperature. The speed of 240 in./min was selected as the maximum speed that could be implemented in current practice [19]. The dipping angles of 1° and 15° were chosen for investigation as practical minimum and maximum values. A minimum angle is necessary during extraction to allow liquid zinc to drain from the part being galvanized, while maximum dipping angle is limited by the kettle depth.



**Figure 10. Evolution of temperature and deformation: (a) temperature in Model 1, (b) Deformation in Model 1, (c) Deformation in Model 5, (d) Deformation in Model 8. All deformations shown amplified 10x.**



**Figure 11. Effect of galvanizing practices on the final deformed shapes: (a) Model 1, (b) Model 5, (c) Model 6, (d) Model 7, and (e) Model 8. All deformations shown amplified 20x.**

Figure 12 shows the calculated measures of distortion as a function of dipping speed and dipping angle. As illustrated, increasing dipping speed significantly reduced web out-of-flatness, slightly reduced twisting, and had a small effect on flange warpage. The level of flange warpage seemed to be induced primarily by the welding process and not by galvanizing. Similarly, increasing the dipping angle reduced out-of-flatness and twisting, but not the warpage, as shown in Figure 13.

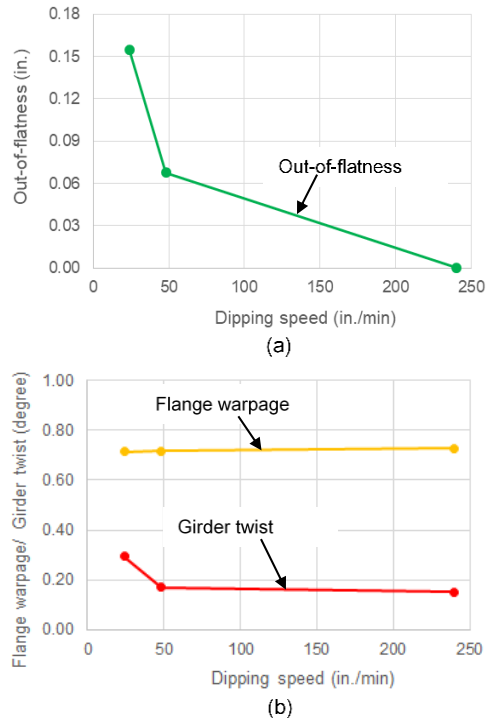


**Figure 12. Effect of dipping speed on (a) out-of-flatness and (b) flange warpage and girder twist.**

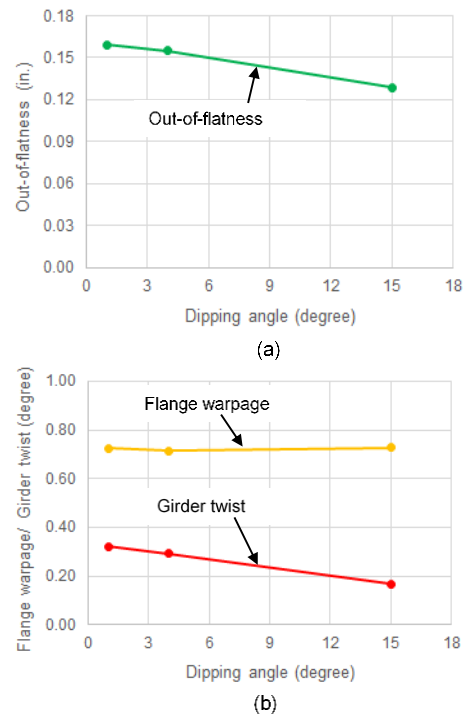


**Figure 13. Effect of dipping angle on (a) out-of-flatness and (b) flange warpage and girder twist.**

## Potential of cracking caused by large distortions during the galvanizing process

On occasion, incidents of cracking have occurred in galvanized steel structures that appear to be induced during the galvanizing process [19-22]. This study has shown that there is a potential for large deformations in plate girders during galvanizing, and that the magnitude of the deformations depends on girder geometry and galvanizing practices. A portion of the deformation was inelastic, which is associated with a greater potential for cracking. Inelastic deformations due to thermal shock are of particular concern in structures exposed to other factors that contribute to the potential for cracking.

Figure 14 shows the change in equivalent plastic strain (PEEQ) in Model 3 as the plate girder was subjected to the simulated hot-dip galvanizing process. The PEEQ values provide a measure of how much cumulative plastic strain the girder sustained during dipping; these values do not include the PEEQ that arose from the welding process, which are much greater in magnitude. Model 3 (the model with 1 ¼ in. thick flanges) was selected because it experienced large deformations during and after the galvanizing process. The girder sustained high levels of accumulated plastic strain of 3,000  $\mu\epsilon$  along a length “A-A”, which was a line of nodes slightly removed from the web-to-flange weld. A peak PEEQ equal to 10,000  $\mu\epsilon$  occurred at the left end of the weld, the result of significant twisting and web buckling during and after the thermal cycles of the galvanizing process.

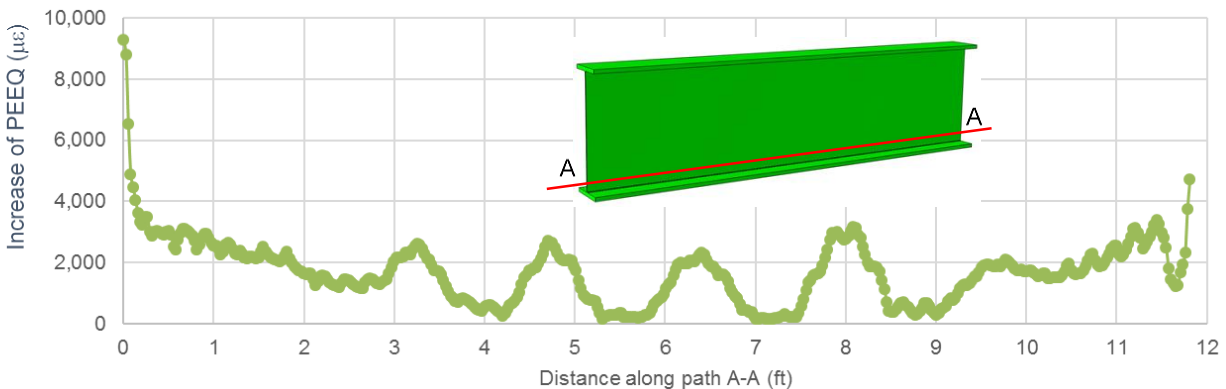


**Figure 14. Increase of equivalent plastic strain, PEEQ, after the galvanizing process in Model 3.**

## Conclusions and Future Work

A study that included eight numerical simulations that captured the effects of welding and hot-dip galvanizing processes on plate girders was presented. The distortion behavior of welded plate girders during and after the hot-dip galvanizing process was illustrated by quantifying web buckling, flange distortion, and girder twisting for the different models. The results showed that increasing flange thickness in the course of this study exacerbated distortion effects, while increasing web thickness was very effective in reducing web buckling and twisting.

The AGA’s recommendation of the flange-to-web thickness ratio of 3 or less was found to be adequate for limiting permanent deformations within acceptable limits based on the results of the models in this study. Regarding galvanizing practices, it is recommended to increase dipping speed and dipping angle as much as practically possible to reduce distortions associated with the galvanizing process. Further work will focus on broadening the studies to other parameters related to the welding process and geometry of the plate girders, such as inclusion of transverse stiffeners, and comparisons of the model results

to physical observations of deformations caused by galvanizing.

## References

- [1] Association, A. G., "Hot-Dip Galvanized Steel Bridges: A Practical Design Guide", A.G. Association, Editor. 2017.
- [2] ASTM A384/A384M – 07 (Reapproved 2013), *Standard Practice for Safeguarding Against Warpage and Distortion During Hot-Dip Galvanizing of Steel Assemblies*, ASTM International, West Conshohocken, PA, 2013, [www.astm.org](http://www.astm.org)
- [3] Cresdee, R. B., Edwards, W. J., Thomas, P. J., and Voss, G. F., "Analysis of beam distortion during hot dip galvanising," *Materials Science and Technology*, Vol. 9, 1993, pp. 161-167, <http://dx.doi.org/10.1179/mst.1993.9.2.161>
- [4] Peric, M., Tonkovic, Z., Rodic, A., Surjak, M., Garasic, I., Boras, I., and Svaic, S., "Numerical analysis and experimental investigation of welding residual stresses and distortions in a T-joint fillet weld," *Materials and Design*, Vol. 53, No. 12, 2014, pp. 1052–1063, <https://doi.org/10.1016/j.matdes.2013.08.011>
- [5] Joosten, M. M. and Gallegillo, M. S., "A Study Of The Effect Of Hardening Model In The Prediction Of Welding Residual Stress," presented at the *ASME 2012 Pressure Vessels & Piping Conference*, Toronto, Ontario, CANADA, 2012, pp. 1045-1054, <https://doi.org/10.1115/PVP2012-78055>
- [6] Simulia, "Abaqus Welding Interface (AWI) - User's Manual". 2017.
- [7] Nguyen, K., Nasouri, R., Bennett, C., Matamoros, A., Li, J., and Montoya, A., "Sensitivity of Predicted Temperature in a Fillet Weld T-Joint to Parameters Used in Welding Simulation with Prescribed Temperature Approach," presented at the *Science in the Age of Experience*, Chicago, IL, USA, 2017, pp. 1-16, <http://web.archive.org/web/20170906023815/https://www.3ds.com/fileadmin/P/RODUCTS/SIMULIA/PDF/scc-papers/2017/temperature-fillet-weld-t-joint-univkansas-nguyen.pdf>,
- [8] Nguyen, K., Nasouri, R., Bennett, C., Matamoros, A., Li, J., and Montoya, A., "Thermomechanical modeling of welding and galvanizing of a steel beam connection detail to examine susceptibility to cracking," *Materials Performance and Characterization*, Vol. In press, 2018, pp.,
- [9] Malik, A. M., Qureshi, E. M., Dar, N. U., and Khan, I., "Analysis of circumferentially arc welded thin-walled cylinders to investigate the residual stress fields," *Thin-Walled Structures*, Vol. 46, 2008, pp. 1391–1401, <https://doi.org/10.1016/j.tws.2008.03.011>
- [10] Dal, M., Le Masson, P., and Carin, M., "A model comparison to predict heat transfer during spot GTA welding," *International Journal of Thermal Sciences*, Vol. 75, 2014, pp. 54-64, <http://dx.doi.org/10.1016/j.ijthermalsci.2013.07.013>
- [11] Higgins, W., "Weld Cracking in Galvanized Steel Structures," Valmont Industries, Inc., 2014, pp.
- [12] Krysl, P., "Finite Element Modeling with Abaqus and Python for Thermal and Stress Analysis," Pressure Cooker Press, San Diego, 2017, pp. 205-207,
- [13] Deng, D. and Murakawa, H., "Prediction of welding distortion and residual stress in a thin plate butt-welded joint," *Computational Materials Science*, Vol. 43, 2008, pp. 353-365, <https://doi.org/10.1016/j.commatsci.2007.12.006>
- [14] Kleineck, J. R., "Galvanizing Crack Formation at Base Plate to Shaft Welds of High Mast Illumination Poles," Master Thesis, 2011, University of Texas, Austin, Texas, <http://web.archive.org/web/20170906023815/https://www.3ds.com/fileadmin/P/RODUCTS/SIMULIA/PDF/scc-papers/2017/temperature-fillet-weld-t-joint-univkansas-nguyen.pdf>

- [015358/https://fsel.engr.utexas.edu/pdfs/KLEINECK-THESIS.pdf](https://fsel.engr.utexas.edu/pdfs/KLEINECK-THESIS.pdf)
- [15] Heinze, C., Schwenk, C., and Rethmeier, M., "Numerical calculation of residual stress development of multi-pass gas metal arc welding," *Journal of Constructional Steel Research*, Vol. 72, 2012, pp. 12 -16,
- [16] Gannon, L., Liu, Y., Pegg, N., and Smith, M., "Effect of welding sequence on residual stress and distortion in flat-bar stiffened plates," *Marine Structures*, Vol. 23, 2010, pp. 385–404,
- [17] Fu, G., Lourenco, M., Duan, M., and Estefen, S., "Influence of the welding sequence on residual stress and distortion of fillet welded structures," *Marine Structures*, Vol. 46, 2016, pp. 30-55,
- [18] *AWS Structural Welding Code—Steel (22nd ed.)*, American Welding Society, Miami, FL, United States of America, 2010,
- [19] Iezawa, T., Yamashita, T., Kanazawa, S., Toi, Y., and Kobashi, K., "Thermal-Elasto-Plastic Analysis on Occurrence of Liquid Zinc Induced Cracking in Bridge Girder under Hot-Dip Galvanizing," *Iron and Steel Institute of Japan*, Vol. 80, No. 12, 1994, pp. 6,
- [20] Feldmann, M., Pinger, T., Tschickardt, D., Bleck, W., Volling, A., and Peter, L., "Analysis of the Influencing Parameters on Cracking Due to Liquid Metal Embrittlement During Hot Dip Galvanizing," *Der Stahlbau*, Vol. 77, No. 1, 2008, pp. 46-61, 10.1002/stab.200810007
- [21] Feldmann, M., Pinger, T., Schafer, D., Pope, R., Smith, W., and Sedlacek, G., "Hot-Dip-Zinc-Coating of Prefabricated Structural Steel Components," Institute for the Protection and Security of the Citizen, Office for Official Publications of the European Communities, 2010, pp. 17-47, <https://doi.org/10.2788/73644>
- [22] Kinstler, T. J., "Current Knowledge of the Cracking of Steels During Galvanizing," GalvaScience LLC,, American Institute of Steel Construction (AISC), 2005, pp. 62-65, <http://web.archive.org/web/20170906014609/https://www.aisc.org/technical-resources/research/researchlibrary/current-knowledge-of-the-cracking-of-steels-during-galvanizing/>